ELECTRONIC SUPPLEMENTARY INFORMATION

Niobium oxide dihalides NbOX_2: a new family of two-dimensional van der Waals layered materials with intrinsic ferroelectricity and antiferroelectricity

Yinglu Jia,[†,‡] Min Zhao,[†] Gaoyang Gou,[*,†] Xiao Cheng Zeng,[*,‡] and Ju Li[*,¶]

†Frontier Institute of Science and Technology, and State Key Laboratory for Mechanical Behavior of Materials, Xi'an Jiaotong University, Xi' an 710049, People's Republic of China

‡Department of Chemistry and Department of Mechanical & Materials Engineering, University of Nebraska-Lincoln, Lincoln, Nebraska 68588, United States

¶Department of Nuclear Science and Engineering and Department of Materials Science and Engineering, Massachusetts Institute of Technology, Cambridge, Massachusetts 02139, United States

E-mail: gougaoyang@mail.xjtu.edu.cn; xzeng1@unl.edu; liju@mit.edu

Crystal structures of bulk NbOX_2

Table S1: Calculated crystallographic parameters for paraelectric (PE) NbOX_2 bulk phases with $C2/m$ (No. 12) symmetry.

PE bulk NbOCl$_2$

a = 6.696 Å, b = 3.825Å, c = 12.569 Å, $\beta = 104.9^{o}$

Atom	x	y	z
Nb (4i)	0.2192	0.0000	0.0001
O (4i)	0.2297	0.0000	0.4965
Cl (4i)	0.0844	0.0000	0.1597
Cl (4i)	0.5696	0.0000	0.1392

PE bulk NbOBr$_2$

a = 7.018 Å, b = 3.834 Å, c = 13.628 Å, $\gamma = 104.1^{o}$

Atom	x	y	z
Nb (4i)	0.2857	0.0000	0.0004
O (4i)	0.2768	0.0000	0.5023
Br (4i)	0.0695	0.0000	0.1355
Br (4i)	0.5861	0.0000	0.1584

PE bulk NbOI$_2$

a = 7.526 Å, b = 3.863 Å, c = 15.053 Å, $\beta = 103.5^{o}$

Atom	x	y	z
Nb (4i)	0.2924	0.0000	0.0006
O (4i)	0.2864	0.0000	0.5009
I (4i)	0.0679	0.0000	0.1298
I (4i)	0.5859	0.0000	0.1562

Table S2: Comparison between the calculated and experimentally measured crystallographic parameters for ferroelectric (FE) NbOX_2 bulk with $C2$ symmetry. Nb polar displacement (d_{Nb}) is measured as the displacement of Nb atom relative to the center of NbO$_2X_4$ octahedra along crystallographic b axis.

FE bulk NbOCl$_2$

Exp:[1] a = 6.686 Å, b = 3.920 Å, c = 12.790 Å, β = 105.3°, d_{Nb} = 0.14 Å

Cal: a = 6.686 Å, b = 3.868 Å, c = 12.520 Å, β = 105.0°, d_{Nb} = 0.15 Å

	Exp[1]			**Cal**		
Atom	x	y	z	x	y	z
Nb (4c)	0.2740	0.0360	0.0000	0.2807	0.0369	0.0003
O (4c)	0.2530	0.5000	0.0000	0.2715	0.5048	0.0017
Cl (4c)	0.0670	0.0000	0.1350	0.0703	-0.0069	0.1391
Cl (4c)	0.5760	0.0000	0.1530	0.5844	-0.0008	0.1600

FE bulk NbOBr$_2$

Exp:[2] a = 7.023 Å, b = 3.908 Å, c = 13.795 Å, β = 104.4°, d_{Nb} = 0.19 Å

Cal: a = 7.010 Å, b = 3.870 Å, c = 13.593 Å, β = 104.1°, d_{Nb} = 0.14 Å

	Exp[2]			**Cal**		
Atom	x	y	z	x	y	z
Nb (4c)	0.2763	0.0005	-0.0003	0.2856	0.0420	-0.0005
O (4c)	0.2740	0.5410	0.0011	0.2780	0.5116	0.0014
Br (4c)	0.0685	0.0535	0.1360	0.0698	0.0001	0.1353
Br (4c)	0.5773	0.0514	0.1514	0.5860	0.0052	0.1586

FE bulk NbOI$_2$

Exp:[3] a = 7.520 Å, b = 3.924 Å, c = 15.036 Å, β = 103.3°, d_{Nb} = 0.14 Å

Cal: a = 7.522 Å, b = 3.896 Å, c = 15.020 Å, β = 103.5°, d_{Nb} = 0.13 Å

	Exp[3]			**Cal**		
Atom	x	y	z	x	y	z
Nb (4c)	0.2900	0.0339	0.0005	0.2923	0.0327	0.0007
O (4c)	0.2898	0.4964	0.0001	0.2872	0.5033	0.0009
I (4c)	0.0682	0.0000	0.1287	0.0676	-0.0047	0.1296
I (4c)	0.5854	0.0007	0.1549	0.5861	-0.0002	0.1565

Table S3: Calculated crystallographic parameters for antipolar $\mathrm{NbO}X_2$ bulk phases with $P2/c$ (No. 13) symmetry.

Antipolar bulk $\mathbf{NbOCl_2}$			
a = 6.686 Å, b = 3.867Å, c = 12.585 Å, β = 105.9^{o}			
Atom	x	y	z
Nb (4g)	0.7807	0.2153	0.2504
O (4g)	0.7715	0.2531	0.7517
Cl (4g)	0.5701	0.7420	0.8890
Cl (4g)	0.0843	0.7479	-0.0901
Antipolar bulk $\mathbf{NbOBr_2}$			
a = 7.010 Å, b = 3.869 Å, c = 13.684 Å, γ = 105.6^{o}			
Atom	x	y	z
Nb (4g)	0.7856	0.2129	0.2505
O (4g)	0.7780	0.2572	0.7515
Br (4g)	0.5694	0.7461	0.8854
Br (4g)	0.0857	0.2486	-0.0914
Antipolar bulk $\mathbf{NbOI_2}$			
a = 7.525 Å, b = 3.895 Å, c = 15.141 Å, β = 105.4^{o}			
Atom	x	y	z
Nb (4g)	0.2924	0.2197	0.2507
O (4g)	0.2873	0.2512	0.7511
I (4g)	0.0676	0.7430	0.8795
I (4g)	0.5869	0.7479	-0.0934

Table S4: Calculated crystallographic parameters for antiferroelectric (AFE) NbOX_2 bulk phases with $P\bar{1}$ (No. 2) symmetry.

AFE bulk NbOCl$_2$

a = 3.861 Å, b = 6.574Å, c = 6.692 Å,
α = 105.0^o, β = 91.0^o, γ = 106.7^o

Atom	x	y	z
Nb (2i)	-0.0309	0.0007	0.7811
O (2i)	0.4997	0.0047	0.7743
Cl (2i)	0.8644	0.7228	0.4302
Cl (2i)	0.8380	0.6794	-0.0851

AFE bulk NbOBr$_2$

a = 3.863 Å, b = 7.014Å, c = 7.109 Å,
α = 104.8^o, β = 105.5^o, γ = 90.8^o

Atom	x	y	z
Nb (2i)	-0.0283	0.2859	0.0010
O (2i)	0.4995	0.2798	0.0033
Br (2i)	0.1337	0.0695	0.2701
Br (2i)	0.1595	0.5863	0.3176

AFE bulk NbOI$_2$

a = 3.891 Å, b = 7.522Å, c = 7.813 Å,
α = 104.7^o, β = 104.2^o, γ = 90.7^o

Atom	x	y	z
Nb (2i)	-0.0268	0.2923	0.0013
O (2i)	0.5002	0.2879	0.0020
I (2i)	0.1271	0.0678	0.2592
I (2i)	0.1569	0.5863	0.3130

Ferroelectric properties of NbOX_2 bulk and monolayer

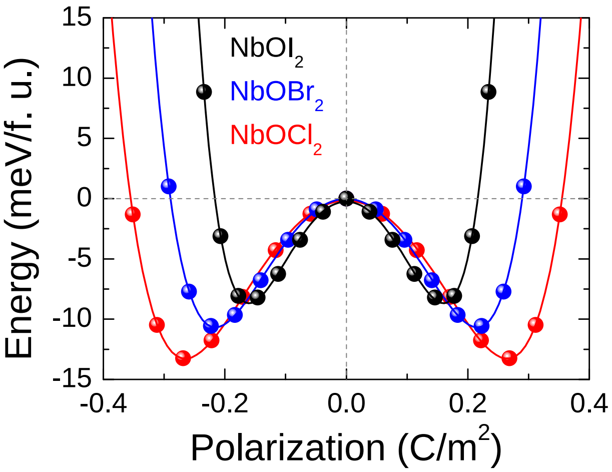

Figure S1: Energy-polarization double well profiles for FE bulk NbOX_2. Energy evolution as a function of spontaneous polarization connecting the FE $C2$ and PE $C2/m$ phases of NbOX_2 bulk. Symbols are the calculated results, and lines are fitted to the data based on Landau model. The trend in magnitude of spontaneous polarization and FE potential depth are NbOI$_2$ < NbOBr$_2$ < NbOCl$_2$.

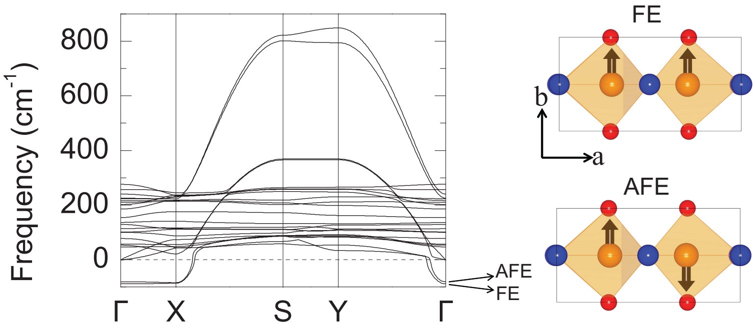

Figure S2: Calculated phonon spectrum for PE NbOI$_2$ monolayer. There are two unstable soft-phonon modes corresponding to ferroelectric (FE) and antiferroelectric (AFE) Nb polar displacement relative to the center of NbO$_2X_4$ octahedra along crystallographic b axis.

Table S5: Calculated imaginary frequencies (in cm^{-1}) for unstable polar phonon modes in PE phases of NbOX_2 bulk and monolayer.

	$NbOCl_2$		$NbOBr_2$		$NbOI_2$	
Phonon mode	bulk	monolayer	bulk	monolayer	bulk	monolayer
FE	i 127.56	i 130.11	i 98.96	i 106.35	i 83.03	i 88.73
antipolar	i 123.00	—	i 96.56	—	i 82.06	—
AFE	i 79.59	i 85.18	i 73.57	i 82.39	i 71.15	i 81.02

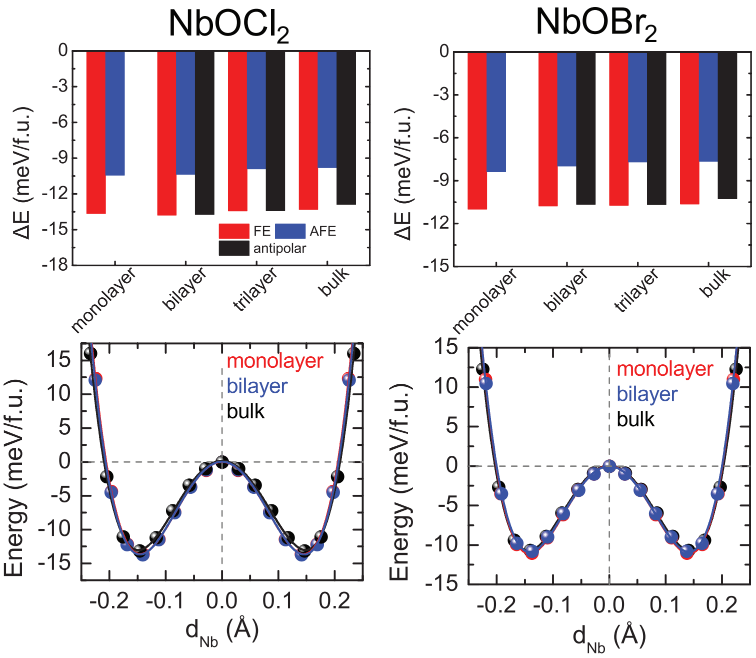

Figure S3: Upper panel: Variation of the total energy for different polar configurations in $NbOCl_2$ and $NbOBr_2$ systems as a function of layer numbers, where the energy of the corresponding PE phases are chosen as energy zero. The energy stability trends are: FE ≈ antipolar > AFE. Lower panel: Nb polar displacement-energy double well plots connecting PE and two FE phases in $NbOCl_2$ and $NbOBr_2$ monolayer, bilayer and bulk. Symbols are the calculated results, lines are fitted to the data based on Landau model. Similar to $NbOI_2$, both the magnitude of Nb polar displacement and spontaneous potential depth in FE $NbOCl_2$ and $NbOBr_2$ remain almost unchanged with respect to the layer numbers.

Optical absorption of bulk NbOX_2

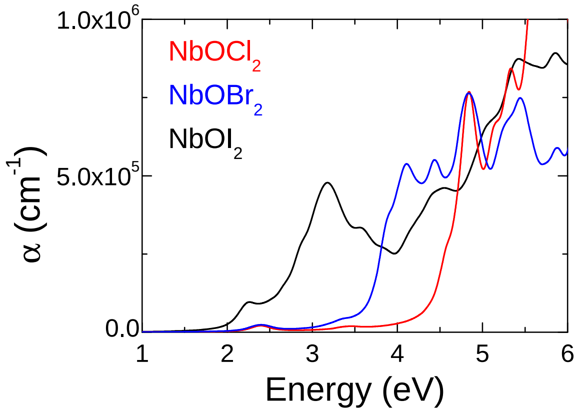

Figure S4: Optical absorption coefficient $\alpha(\omega)$ for FE NbOX_2 bulk, calculated using HSE functional. Among the three bulk compounds, only NbOI_2 exhibits semiconducting optical absorption properties. As an indirect band gap semiconductor, NbOI_2 bulk can effectively absorbs incident light with photon energy above 2.0 eV.

Computational details for MC and MD simulations

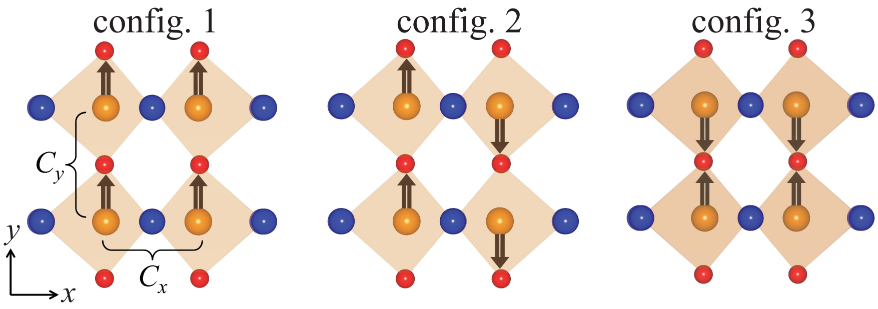

Figure S5: Three different polar configurations used to extract the polar displacement interaction parameters C_x and C_y appeared in Table 2 of the main text. Config. 1 and 2 correspond to FE and AFE phase for NbOX_2 monolayer, Config. 3 contains head-to-head (tail-to-tail) Nb polar arrangement, which is highly unfavorable. We constrain three configurations to have same Nb polar displacement amplitude ($|d_i|=d$). So that based on Eq. (2) of main text, their energy difference can be written as: E_2 - E_1 = $16C_x \cdot d^2$; E_3 - E_1 = $16C_y \cdot d^2$. The obtained parameters $C_y \gg C_x$, owing to the very high energy cost to form head-to-head (tail-to-tail) polar arrangement.

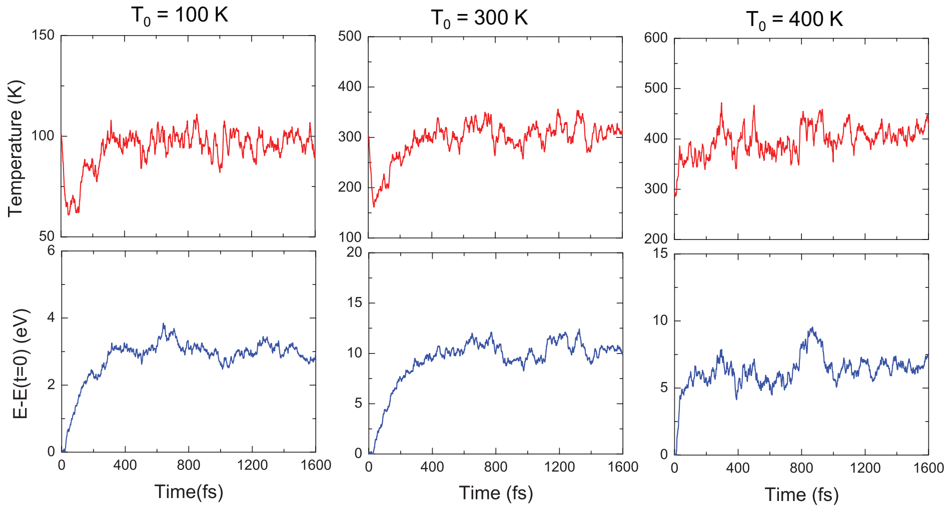

Figure S6: Full time evolution of the instantaneous temperature, total energies for $NbOI_2$ monolayer at the selected target temperature during *ab initial* MD simulations.

MC simulations:

Based on the effective Hamiltonian (Eq. (2) of main text) with parameters given in Table 2 of the main text, we perform MC simulations using the Metropolis algorithm[4] for $NbOX_2$ monolayers. A periodic 2D slab composed of 60 × 60 × 1 of $NbOX_2$ unit cells (corresponding to a supercell containing 7200 Nb lattice grids). Zero temperature FE phase is chosen as the initial state, where Nb cation from each lattice grid carries same d_i. Each MC step starts by randomly changing the magnitude of d_i with any value in the range of [-$|d|$,$|d|$]. The probability for changing the sign of d_i at a given temperature T is determined by

$$\Delta d_i = \begin{cases} exp(-\frac{\Delta E}{k_B T}), & \text{when } \Delta E > 0 \\ 1, & \text{when } \Delta E > 0 \end{cases} \tag{1}$$

where k_B is the Boltzmann constant and ΔE is the energy difference of the system before and after changing the sign of d_i. For simulation of each configuration under different temperature and electric field, we run at least 3000 MC steps to ensure the thermal-equilibrium. And then at least 300 steady MC steps were further used to calculate the macroscopic average polar displacement $<d>$.

Ab initio MD simulations:

We also performed *ab initio* MD simulations implemented in VASP using NVT ensemble at zero pressure and a time step of 1 fs. SCAN+rVV10 functional and same plane-wave basis set, PAW method as zero temperature DFT calculations are used for MD simulations. A 4 × 8 × 1 periodic supercell containing 256 atoms (8 × 8 Nb lattice grid) was used to simulate NbOX_2 monolayers. Full time evolution of the instantaneous temperature, total energies for $NbOI_2$ monolayer at the selected target temperature are shown in Figure S6. We perform MD simulations up to 1.6 ps to ensure the system can reach thermal-equilibrium state. 150 configuration snap-shots around thermal-equilibrium are used for statistics.

Strain engineering of NbOX_2 monolayer

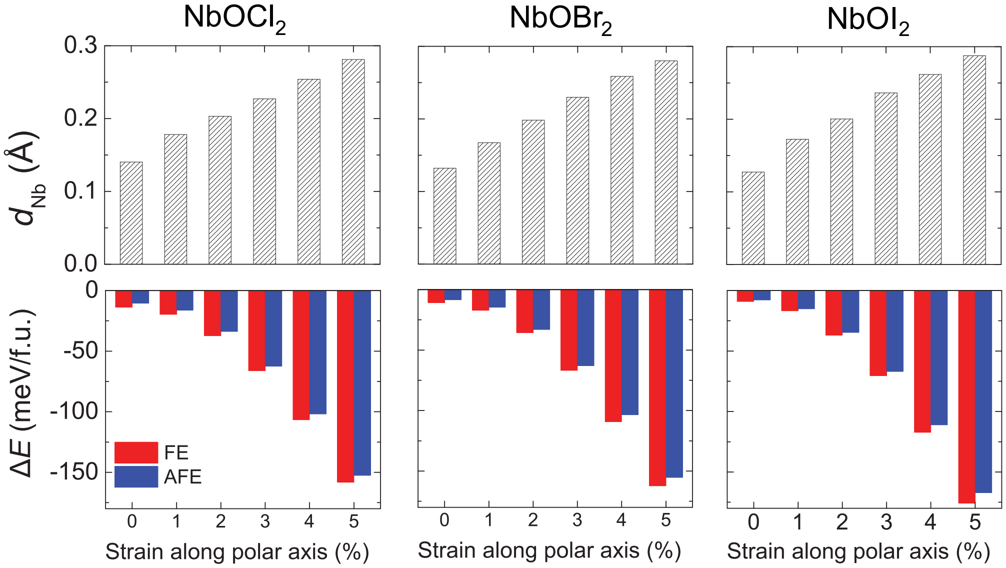

Figure S7: Variation of Nb polar displacement (d_{Nb}) in FE phase, the energy for FE and AFE phases relative to PE phase (ΔE) of NbOX_2 monolayer as a function of tensile strain applied along the polar axis.

References

(1) D. Drobot, and E. Pisarev, *Russ. J. Inorg. Chem.* 1984, **29**, 1561–1563.

(2) J. Beck, and C. Kusterer, *Z. Anorg. Allg. Chem.* 2006, **632**, 2193–2194.

(3) J. Rijnsdorp and F. Jellinek, *J. Less-Common Met.* 1978, **61**, 79–82.

(4) N. Metropolis, A. W. Rosenbluth, M. N. Rosenbluth, A. H. Teller and E. Teller, *J. Chem. Phys.* 1953, **21**, 1087–1092.